Molecular basis of recognition of quadruplexes human telomere and c-myc promoter by the putative anticancer agent sanguinarine

ARTICLE *in* BIOCHIMICA ET BIOPHYSICA ACTA · APRIL 2013

Impact Factor: 4.66 · DOI: 10.1016/j.bbagen.2013.03.027 · Source: PubMed

5 AUTHORS, INCLUDING:

Saptaparni Ghosh
Saha Institute of Nuclear Physics
10 PUBLICATIONS **71** CITATIONS
SEE PROFILE

Anirban Kar
Institute of Genomics and Integrative Biology
8 PUBLICATIONS **112** CITATIONS
SEE PROFILE

Biochimica et Biophysica Acta 1830 (2013) 4189–4201

Contents lists available at SciVerse ScienceDirect

Biochimica et Biophysica Acta

journal homepage: www.elsevier.com/locate/bbagen

Molecular basis of recognition of quadruplexes human telomere and c-myc promoter by the putative anticancer agent sanguinarine

Saptaparni Ghosh [a], Suman Kalyan Pradhan [a,1], Anirban Kar [b], Shantanu Chowdhury [b], Dipak Dasgupta [a,*]

[a] Biophysics Division, Saha Institute of Nuclear Physics, Block-AF, Sector-I, Bidhan Nagar, Kolkata-700064, India
[b] Proteomics and Structural Biology Unit, Institute of Genomics and Integrative Biology, CSIR, Room No. 307, Mall Road, Delhi-110007, India

ARTICLE INFO

Article history:
Received 31 January 2013
Received in revised form 19 March 2013
Accepted 26 March 2013
Available online 4 April 2013

Keywords:
Sanguinarine
Human telomeric DNA
NHE III_1 upstream of the P1 promoter of c-myc
Fluorescence and CD spectroscopy
Calorimetry
Telomerase repeat amplification protocol

ABSTRACT

Background: Interaction of putative anticancer agent sanguinarine with two quadruplex forming sequences, human telomeric DNA (H24) and NHE III_1 upstream of the P1 promoter of c-myc (Pu27), has been studied to understand the structural basis of the recognition.
Methods: Absorption, fluorescence and circular dichroism spectroscopy have been employed to characterize the association. Energetics of the interaction was studied by isothermal titration and differential scanning calorimetry. TRAP assay was done to assess the inhibitory potential of sanguinarine.
Results: Absorption and fluorescence studies show that sanguinarine has high binding affinity of ~10^5 M^{-1} for both sequences. Binding stoichiometry is 2:1 for H24 and 3:1 for Pu27. Results suggest stacking interaction between planar sanguinarine moiety and G-quartets. Circular dichroism spectra show that sanguinarine does not cause structural perturbation in the all-parallel Pu27 but causes a structural transition from mixed hybrid to basket form at higher sanguinarine concentration in case of H24. The interaction is characterized by total enthalpy–entropy compensation and high heat capacity values. Differential scanning calorimetry studies suggest that sanguinarine binding increases the melting temperature and also the total enthalpy of transition of both quadruplexes. TRAP results show that sanguinarine effectively blocks telomerase activity in a concentration dependent manner in cell extracts from MDAMB-231 breast cancer cell lines.
Conclusion: These results suggest that there is a difference in the structural modes of association of sanguinarine to the quadruplexes.
General significance: It helps to understand the role of quadruplex structures as a target of small molecule inhibitors of telomerase.

1. Introduction

DNA is considered to be a duplex molecule in which two self complimentary strands are held together by Watson–Crick base pairs. Depending upon the DNA sequence, alternative conformations such as triple helix [1], Holliday-junction [2], hairpin [3,4] *etc.* are possible. Certain purine rich DNA sequence which contains runs of guanine can fold into four stranded structures known as G-quadruplexes [5–7]. The uniqueness of G-quadruplexes lies in their structure where series of stacked guanine tetrad are held together in a coplanar cyclic array by both Hoogsteen and Watson–Crick hydrogen bonds [6,8].

Polyguanine sequences are known to fold into G-quadruplex structures *in vitro*, in the presence of monovalent cations like Na^+ or K^+ [9–11]. Depending on the type of counterion, incubation period and sequence being used, the quadruplex may adopt either of the following geometries: parallel, antiparallel or mixed parallel and antiparallel [9–11]. There have been circular dichroism [12–14] and NMR [10,13,15,16] studies to identify and distinguish among the conformations which a quadruplex adopts.

In vivo, such sequences are found in the telomeric region of chromosomes and transcription regulatory region of several oncogenes [17–20]. In line with our initial observations suggesting role of G-quadruplex motifs in gene regulation in prokaryotes [21] more recent findings indicate such possibility not only in humans but also in chimpanzee, mouse and rat [22,23]. Further support for direct involvement in gene regulation was obtained from a study showing that a regulatory factor NM23-H2 engaged a G-quadruplex motif for regulation of the oncogene c-myc

Abbreviations: SGR, sanguinarine; H24, human telomeric DNA; Pu27, NHE III_1 upstream of the P1 promoter of c-myc; CD, circular dichroism; ITC, isothermal titration calorimetry; DSC, differential scanning calorimetry; TRAP, telomerase repeat amplification protocol

* Corresponding author at: Dipak Dasgupta, Biophysics Division, Saha Institute of Nuclear Physics, Block-AF, Sector-I, Bidhan Nagar, Kolkata 700064, India. Tel.: +91 33 23375345 49x3114; fax: +91 33 23374637.
E-mail address: dipak.dasgupta@saha.ac.in (D. Dasgupta).
[1] Present Address: Department of Biological Chemistry, David Geffen School of Medicine, University of California, Los Angeles, CA, USA.

0304-4165/$ – see front matter © 2013 Elsevier B.V. All rights reserved.
http://dx.doi.org/10.1016/j.bbagen.2013.03.027

[24]. In addition, various other proteins that can recognize, bind or resolve G-quadruplex motifs were subsequently identified which provide support for the presence of these structures *in vivo* [25–28].

The enzyme telomerase, which is absent in normal somatic cells but present in 85–90% of cancer cells adds the telomeric repeat unit (TTAGGG in case of humans) to the ends of the chromosome contributing to their immortality [29–31]. The telomeric region of the chromosome must remain single stranded for telomerase to add the telomeric repeat unit [32]. Thus, uncontrolled cellular proliferation can be arrested by either blocking telomerase directly or by making the telomerase substrate inaccessible.

Studies based upon bioinformatics have shown that there are ~376,000 potential G-quadruplex forming motifs in the human genome [19,20]. These motifs were noted to be abundant in the promoter region of genes especially near the transcription start site (c-myc, c-kit, c-myb, KRAS, PDGF-A, VEGF, BCL-2, MyoD, HIF-1α and TK1) suggesting a role of quadruplex structures in transcription [33]. Among these the quadruplex in the promoter region of c-myc has been widely studied. The guanine rich nuclear hypersensitivity element III_1 (NHE III_1), upstream of the P1 promoter of c-myc proto-oncogene (which is overexpressed in 60–80% of all cancers), can fold into an intramolecular G-quadruplex structure and control about 80–90% of its transcription [34–38]. Overexpression of c-myc results in an increase in cellular proliferation and cell growth and has been shown to influence and inhibit normal cell cycle [36,39].

There has been a surge in the reports of small molecules with potential to bind to quadruplex structures thereby stabilizing them [40–56]. These molecules can act as effective anticancer agents by stabilizing the telomeric regions of DNA or by regulating gene expression of oncogenes. Some of these molecules also induce the formation of quadruplex structures in G-rich sequences [57,58]. But until recently, the energetics of these interactions has not been well studied. Here we have characterized the binding of a naturally occurring plant alkaloid, sanguinarine (SGR), isolated from *Sanguinaria canadensis* with therapeutic potential [59] and ability to bind to quadruplex structure [60,61], with the human telomeric DNA sequence (H24) and the NHE III_1 upstream of the P1 promoter of c-myc (Pu27) (Table 1).

SGR (Fig. 1) exists in two forms, the positively charged iminium form and the neutral alkanolamine form, in aqueous medium near physiological pH. While the iminium form (pH 1–6) is unsaturated and completely planar, the alkanolamine (pH 8.5–11) form has a buckled structure. Earlier reports have shown that, although the iminium form interacts with B-form DNA, the alkanolamine form does not [62].

In the presence of K^+ ions, the two sequences we have chosen fold differently. An intramolecular parallel quadruplex is formed by crystals of human telomeric DNA sequence in K^+ ions [63]. But the solution structure of the sequence has been shown to be different from its crystal structure by in solution biophysical methods. Several studies using NMR [64,65], CD [66] and fluorescence spectroscopy and sedimentation equilibrium and velocity experiments [67] have proved that the sequence in K^+ solution is a mixture of multiple conformers like basket, chair, (3 + 1) hybrid 1 and (3 + 1) hybrid 2. All these four conformers

Table 1
Oligomers used in the present studies.

Oligomer	Sequence
Human telomeric DNA (H24)	5′-TTAGGGTTAGGGTTAGGGTTAGGG-3′
Complementary human telomeric DNA (H24rev)	5′-CCCTAACCCTAACCCTAACCCTAA-3′
NHE III_1 upstream of the P1 promoter of c-myc (Pu27)	5′-TGGGGAGGGTGGGGAGGGTGGGGAAGG-3′
Complementary NHE III_1 upstream of the P1 promoter of c-myc (Pu27rev)	5′-CCTTCCCCACCCTCCCCACCCTCCCCA-3′
Pu121 (1:2:1 isomer of Pu27)	5′-TTTTTAGGGTGGGGAGGGTGGGGAAGG-3′
Pu161 (1:6:1 isomer of Pu27)	5′-TGGGGAGGGTTTTTAGGGTGGGGAAGG-3′

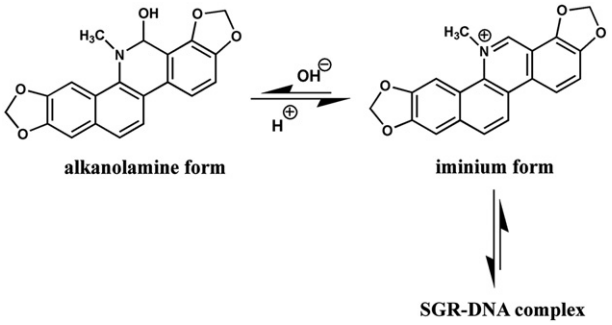

Fig. 1. Iminium and alkanolamine forms of sanguinarine (SGR). The iminium form binds to DNA.

have a mixed parallel–antiparallel structure. The major structure which the sequence adopts depends on the presence/absence and nature of flanking bases at the 5′ and 3′ end of the quadruplex forming region and the input concentration of K^+ ions. NMR studies on a number of modified human telomeric sequences have shown that H24 folds into the (3 + 1) hybrid structure rather than the chair or basket form in K^+ ions [64,65,68,69]. NMR studies have shown that the modified 24 nucleotide sequence, 5′-[TTGGG$(TTAGGG)_3$A]-3′, folds into the (3 + 1) hybrid 1 structure which is stabilized over the other structures by the formation of Watson–Crick base pairing between T1 and A20 [64]. Similar hydrogen bond formation between T2 and A21 of H24 sequence is feasible and favors the formation of the (3 + 1) hybrid 1 structure over other antiparallel structures, though minor amounts of (3 + 1) hybrid 2 structure maybe present. In an earlier report from our laboratory on SGR-H24 interaction [61], we have also shown using Convex Constraint Analysis (CCA) that the (3 + 1) hybrid 1 is the major conformer of H24 in presence of K^+ ions with minor amounts of (3 + 1) hybrid 2 conformer. Results from various experiments lead us to conclude that the major conformation which H24 adopts in K^+ ions is the (3 + 1) hybrid 1 form with minor amounts of (3 + 1) hybrid 2 form. Contrary to H24 which adopts a mixed parallel–antiparallel structure [64,65,68], Pu27 adopts a parallel structure [70,71].

In this study we have used different spectroscopic and calorimetric techniques to elucidate and understand the structural and energetic aspects of SGR binding to two structurally different quadruplex structures.

2. Materials and methods

2.1. Materials and preparation of stock solutions

SGR, sodium acetate, acetic acid, potassium phosphate monobasic, potassium phosphate dibasic, calf thymus DNA (ct DNA) and desalted and HPLC purified oligomers-H24, H24rev, Pu27, Pu27rev and mutant Pu27 (Pu121 and Pu161) (Table 1) were purchased from Sigma Chemical Corporation, USA. H24rev and Pu27rev are the complementary sequences of H24 and Pu27. All buffers were prepared in MilliQ water from Millipore Water System, Millipore, USA and filtered through 0.1 μm filters from Millipore, USA prior to use.

SGR was dissolved in 10 mM pH 5.2 sodium acetate buffer and kept overnight at 4 °C. The concentration of the stock drug solution was determined from absorbance using $\varepsilon_{327\ nm} = 30{,}700\ M^{-1}\ cm^{-1}$.

To prepare quadruplex the oligomers (H24, Pu27 and mutant Pu27) were dissolved in 10 mM potassium phosphate buffer pH 6.8 containing 150 mM KCl and heated to 90 °C in a water bath and kept for 10 min. The samples were allowed to equilibrate slowly to room temperature and stored at 4 °C for 48 h. They were dialyzed against the same buffer for 24 h. The concentrations of the oligomers were determined by absorbance measurement using $\varepsilon_{260\ nm} =$

244,600 M^{-1} cm^{-1}, 279,900 M^{-1} cm^{-1} and 272,700 M^{-1} cm^{-1} for H24, Pu27 and mutant Pu27 (Pu161 and Pu121) respectively. The molar extinction coefficient values of the oligomers were determined using nearest neighbor approximation model. The purity of the oligomers were confirmed by the appearance of a single band for the oligomers in a 20% native PAGE. Characteristic CD spectra of the oligomers confirmed the formation of (3 + 1) hybrid structure for H24 [72] and parallel structure for Pu27 [12,73]. All experiments were carried out in 10 mM potassium phosphate buffer, pH 6.8, containing 150 mM KCl. Under this buffer condition, SGR exists in the charged iminium form and it is this form that interacts with quadruplex and duplex DNA used in this study.

In order to prepare the corresponding duplex strands of H24 and Pu27, the respective oligomers and their complementary strands (Table 1) were dissolved individually in 10 mM potassium phosphate buffer pH 6.8 and heated to 90 °C and kept for 10 min. The samples were cooled slowly and concentration was determined by absorbance measurement using $\varepsilon_{260\ nm}$ = 220,400 and 215,200 M^{-1} cm^{-1} for H24rev and Pu27rev respectively. The oligomers and their corresponding complementary strands were mixed in equal molar ratio and heated to 90 °C and kept for 10 min. The samples were cooled slowly and concentration was determined by absorbance measurement using $\varepsilon_{260\ nm}$ = 384,555 and 436,623.2 M^{-1} cm^{-1} for H24 duplex and Pu27 duplex respectively.

ct DNA was deproteinized by phenol–chloroform extraction method and precipitated with ethanol. It was then dissolved in 10 mM pH 6.8 potassium phosphate buffer and dialyzed against the same buffer. The concentration of ct DNA was determined by absorbance measurement using $\varepsilon_{260\ nm}$ = 6600 M^{-1} cm^{-1}.

2.2. Absorption and fluorescence spectral studies

Absorption spectra were measured in CECIL 7500 UV-visible spectrophotometer. 10 μM of SGR was titrated with increasing amount of H24 and Pu27 until saturation was reached (equal amount of DNA was added to the reference cell during titration) to determine the dissociation constant of the interaction. Saturation was reached at 13.14 and 14.33 μM for H24 and Pu27, respectively. Readings were noted 5 min after each addition to ensure complete complex formation. The binding isotherm was generated by plotting $\Delta A / \Delta A_{max}$ at 327 nm as a function of added quadruplex concentration. The experimental points for the binding isotherm were fitted using the equation [74]

$$C_0(\Delta A/\Delta A_{max})^2 - \left(C_0 + C_p + K_d\right)(\Delta A/\Delta A_{max}) + C_p = 0 \quad (1)$$

where C_0 is the initial concentration of SGR, ΔA is the change in absorbance at 327 nm for each addition of quadruplex, ΔA_{max} is the same parameter when SGR is totally bound to quadruplex and C_p is the concentration of quadruplex added. The X-intercept value at $\Delta A / \Delta A_{max}$ = 0.5 (corresponding to 50% binding) gives the dissociation constant, K_d. ΔA_{max} was determined from the double reciprocal plot of 1 / ΔA against 1 / (C_P − C_0) using the equation [74]

$$1/\Delta A = 1/\Delta A_{max} + 1/\left(C_p - C_0\right). \quad (2)$$

Binding stoichiometry was obtained from the break in the straight lines resulting from the above plot. The concentration of quadruplex at the break was divided by the SGR concentration to obtain the binding stoichiometry.

The method of continuous variation (Job Plot) was also employed to determine the binding stoichiometry of SGR binding to H24 and Pu27 [75]. Absorbance of SGR was recorded at 327 nm for reaction mixtures, in which number of moles of H24/Pu27 and SGR in a fixed volume were varied, keeping the sum total number of moles constant. Absorbance of SGR was plotted as a function of the input mole fraction of quadruplex. The point in the plot where the resulting two straight lines meet, corresponds to the mole fraction of quadruplex in the quadruplex:SGR complex. The stoichiometry is obtained in terms of

$$\text{quadruplex} : \text{SGR} = \chi_{\text{quadruplex}} : \left(1 - \chi_{\text{quadruplex}}\right) \quad (3)$$

where $\chi_{\text{quadruplex}}$ is the mole fraction of quadruplex calculated as the ratio of the molar concentration of quadruplex to the total molar concentration of quadruplex and SGR.

Fluorescence anisotropy was recorded on a Perkin Elmer, LS 55 Luminescence Spectrometer. The excitation and emission wavelengths were fixed at 327 and 570 nm respectively for SGR. The excitation and emission slits were fixed at 5 nm and 10 nm respectively. Each reading was an average of eight runs. Readings were noted 5 min after each addition to ensure complete complex formation. Anisotropy was calculated using the equation [76]

$$r = (I_{VV} - GI_{VH})/(I_{VV} + 2G.I_{VH}) \quad (4)$$

where I denotes the intensity and the subscripts refer to the vertical or horizontal positioning of excitation and emission polarizers respectively.

$$G = I_{HV}/I_{HH} \quad (5)$$

is the instrumental correction factor, used to correct for polarizing effects in the emission monochromator and detector [77]. Anisotropy values were plotted as a function of increasing quadruplex concentration and the association constants were obtained by fitting the data to the Hill Equation using Origin 7.0. Final concentration of H24 and Pu27 was 12.64 and 7.42 μM, respectively.

2.3. Isothermal titration calorimetry

ITC experiments were done in iTC200 Microcalorimeter, Microcal Inc., USA at different temperatures between 10 °C and 35 °C. Samples were extensively degassed prior to titration. Titration of SGR against G-quadruplex was performed by injecting G-quadruplex into a fixed concentration of SGR (10 μM). Final concentration of H24 and Pu27 was 11.30 and 13.04 μM, respectively. The heat released due to the addition of aliquots of quadruplex to the drug solution was measured by a thermoelectric device between the sample and reference cells. The heat associated with each injection was observed as a peak which corresponds to the power required to maintain the sample and reference cells at identical temperatures. The peaks produced over the course of the titration can be converted to heat output per injection by integration and correcting for cell volume and sample concentration. The heat released for the i-th injection, ΔQ(i) is given by [78]

$$\Delta Q(i) = Q(i) + \frac{dV_i}{V_0}\left[\frac{Q(i) + Q(i-1)}{2}\right] - Q(i-1) \quad (6)$$

where V_i is the injection volume and V_0 is the cell volume. The total heat released (Q(t)) was fitted by a non-linear least square minimization method using the equation [78]

$$Q(t) = \frac{nM_t\Delta HV_0}{2}\left[1 + \frac{X_t}{nM_t} + \frac{1}{nkM_t} - \sqrt{\left(1 + \frac{X_t}{nM_t} + \frac{1}{nkM_t}\right)^2 - \frac{4X_t}{nM_t}}\right] \quad (7)$$

where n is the number of binding sites, k is the binding constant, M_t is the bulk concentration of macromolecule in active cell volume (V_0), X_t is the bulk concentration of the ligand and ΔH is the molar heat of ligand binding. A blank experiment in which G-quadruplex was injected into buffer with no SGR was carried out to correct the data due to dilution. Background was subtracted from the measured heats, and the corrected heats were plotted against molar ratio. The

corrected isotherms showed that only one type of binding event is taking place in both the cases. The isotherms were analyzed using the in-built Microcal LLC ITC software. 'One set of sites' model yield the best fitted curve for the obtained data points. Equilibrium association constant (K_a), enthalpy (ΔH) and entropy (ΔS) of association were obtained after fitting each isotherm. Gibbs energy was calculated using the equation

$$\Delta G = \Delta H - T\Delta S. \quad (8)$$

Change in heat capacity (ΔC_p) for the association of SGR with G-quadruplex was calculated from the slope of the plot of enthalpy change (ΔH) against temperature. To determine the extent of enthalpy–entropy compensation the slope of ΔH versus $T\Delta S$ was determined for both interactions.

25 μM SGR was titrated by injecting H24 duplex, Pu27 duplex and ct DNA until saturation was reached. The final concentration of H24 duplex and Pu27 duplex was 11.93 μM and ct DNA was 24.86 μM. The thermogram was analyzed using the 'one set of sites' model to determine the association constant for the interaction at 25 °C. To maintain the ionic strength of the solution, 150 mM KCl was added to the buffer prior titration.

2.4. Circular dichroism studies

Circular dichroism spectra were recorded on a JASCO J715 spectropolarimeter (Jasco Cooperation, Tokyo, Japan) at 25 °C. The CD scans were recorded within the wavelength range of 220–360 nm with scan speed 200 nm/min and step size of 0.1 nm. The time constant was 2 s and bandwidth was 1 nm. All measurements were carried out in a 0.1 cm path length cuvette in a reaction volume of 300 μL. Fixed amount of quadruplex (10 μM Pu27) was titrated with increasing concentration of SGR. Each reading was an average of four runs. Readings were noted 5 min after each addition to ensure complete complex formation. Convex constraint analysis (CCA) was performed on the spectral set in order to extract the basis spectra and their associated coefficients [79].

2.5. Differential scanning calorimetry

The excess heat capacity was measured as a function of temperature in a VP DSC Microcalorimeter (Microcal, LLC, Northampton, MA) to investigate the helix to coil transition. The samples were scanned from 10 °C to 120 °C in case of H24–SGR and from 10 °C to 130 °C in case of Pu27–SGR, at a scan speed of 60 °C/h at approximately 25 psi pressure. Prior to sample scan, the instrument was thermally stabilized by repeated buffer scans under similar conditions. 100 μM of quadruplex was scanned to obtain the melting profile of the unbound forms. 70 μM of quadruplex was incubated with 190 μM of SGR in case of H24 and 260 μM of SGR in case of Pu27, Pu121 and Pu161 for one hour to ensure complete complex formation and scanned to obtain the melting profile of the bound forms. The thermograms obtained were analyzed using the in-built VPViewer software with Origin 7.0. The non-2-state (cursor initiation) model of curve fitting was used to fit the raw thermograms. Since $\Delta S^0 = \Delta[(\Delta C_p / T) / \Delta T]$, the area under the $\Delta Cp / T$ versus T plot yields ΔS^0. The Gibbs free energy was calculated using Eq. (8), once the enthalpy and entropy values were determined at 25 °C.

2.6. Telomerase Repeat amplification Protocol

The SYBR Green RQ-TRAP assay was conducted with cell extracts from MDAMB-231 breast cancer cell lines in 25 μL of reaction mixture with SYBR Green PCR Master Mix (US Biomax, INC-Telomerase Detection Kit-MT3012). Quantitative real time PCR was done to study the *in vitro* effect of SGR on telomerase activity. Using ABI7500 Fast Real Time PCR, USA samples were incubated at 25 °C for 20 min and amplified in 40 PCR cycles with 30 s at 95 °C, 30 s at 60 °C and 30 s at 72 °C (three-step PCR). PCR amplification occurs in the second step of the PCR cycle. In this step telomerase (from the cell extract) adds the telomeric repeat unit (TTAGGG) to the 3′-end of the TS primer (AATCCGTCGAGCAGAGTT) present in the master mix. Fluorescence data was collected in the third PCR step. The threshold cycle values (C_t) were determined from the semi-log amplification plot. C_t denotes the number of PCR cycles after which detectable fluorescence intensity is observed. RQ-TRAP assay was done with 0, 2, 4, 5 and 8 μM SGR keeping the reaction mixture volume fixed (25 μL). Each sample was analyzed in triplicate. The obtained C_t values at different SGR concentrations give an idea about the telomerase activity in the cell extract. From the observed C_t values we can calculate the transformed fold change in telomerase activity with varying SGR concentrations. Transformed fold change in telomerase is calculated as follows

$$\Delta C_t = C_{t,c} - C_{t,0} \quad (9)$$

where $C_{t,c}$ is the average C_t value for a particular concentration (c μM) of SGR and $C_{t,0}$ is the average C_t value for 0 μM of SGR.

$$\text{Fold change in telomerase activity due to presence of SGR, X} = 2^{(-\Delta C_t)}. \quad (10)$$

$$\text{Transformed fold change} = 1/X \quad (11)$$

3. Results

3.1. Absorption and fluorescence studies

Association of H24 and Pu27 with SGR was demonstrated by absorbance spectroscopy. Insets of Fig. 2A and B show that on binding to quadruplex the absorbance of SGR at 327 nm decreases accompanied by a red shift of the peak by about 10 nm and appearance of an isosbestic point at 370 nm. The presence of an isosbestic point indicates the presence of a single type of quadruplex: SGR complex over the input concentration range of quadruplex. Similar results have been reported for several other small molecules that bind to G-quadruplex structures [50,60,80,81]. Change in absorbance of SGR at 327 nm was plotted as a function of increasing quadruplex concentration and analyzed according to the method stated earlier to determine the dissociation constants (Fig. 2A and B). SGR binds strongly to both sequences as evident from Table 2 with a relatively higher affinity for H24. A break at 0.36 and 0.25 mole fractions of quadruplex in Job's Plot (Fig. 2C and D) indicates a 1:2 and 1:3 binding for H24 and Pu27 respectively, with SGR. In contrast to our results, Bhadra et al. [60] proposed that SGR binds to H22 with 1:1 binding stoichiometry.

Additional support for the association of quadruplex with SGR is obtained from decrease in the fluorescence emission spectra (data not shown) and increase in fluorescence polarization anisotropy (FPA) of SGR on addition of increasing concentrations of quadruplex. Binding of SGR to quadruplex reduces its mobility resulting in an increase of anisotropy of SGR in the bound form. On binding to H24 the anisotropy value of SGR increases from 0.008 to 0.117 corresponding to a 14.6-fold increase when SGR is completely complexed with H24 (Fig. 3A). In case of Pu27 the anisotropy value of SGR increases from 0.008 to 0.132 corresponding to a 16.5-fold increase when SGR is completely complexed with Pu27 (Fig. 3B). The dissociation constant values determined from FPA are summarized in Table 2.

3.2. Isothermal titration calorimetric studies

ITC experiments were done at different temperatures to determine the thermodynamic parameters for the interaction of SGR with both sequences. Measurement of the thermodynamic parameters at different

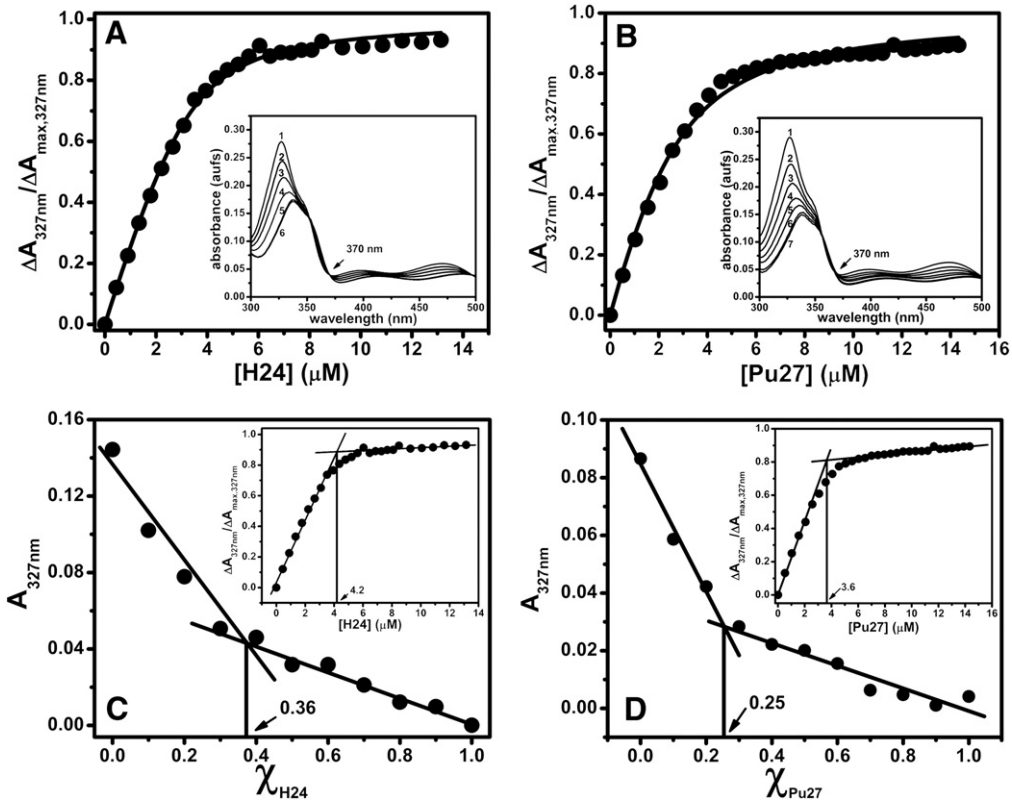

Fig. 2. Curve fitting analysis of the binding isotherm obtained from absorption titration to evaluate the dissociation constant for the association of SGR (10 μM) with (A) H24, *Inset:* Absorption spectra (300–500 nm) of SGR (1) in presence of increasing concentration (0.89, 1.78, 3.09, 7.28, 10.07 μM) of H24 (2–6) and (B) Pu27, *Inset:* Absorption spectra (300–500 nm) of SGR (1) in presence of increasing concentration (1.04, 2.06, 3.07, 4.07, 10.29, 13.89 μM) of Pu27 (2–7). Job Plot to determine the binding stoichiometry for association of SGR to (C) H24 *Inset:* Binding stoichiometry obtained from the break in the straight lines representing the linear fit of the initial and final few data points of the absorption titration curve and (D) Pu27 *Inset:* Binding stoichiometry obtained from the break in the straight lines representing the linear fit of the initial and final few data points of the absorption titration curve. All experiments were done at 25 °C in 10 mM potassium phosphate buffer (pH 6.8) containing 150 mM KCl.

temperatures enabled us to determine the extent of enthalpy–entropy compensation and also the heat capacity change as a sequel to association for both quadruplexes. The representative thermograms for the binding are shown in Fig. 4A and B. The binding parameters obtained from ITC are summarized in Table 3.

In both cases enthalpy and entropy contribute favorably towards the association. In both the systems, the enthalpy and entropy value of the reaction decreases with increasing temperature keeping the free energy of the association almost invariant with temperature. The slope of ΔH versus TΔS for H24-SGR interaction is 0.90 ± 0.06 (Fig. 4E) and for Pu27-SGR interaction is 1.04 ± 0.03 (Fig. 4F). Linear relationship of ΔH with TΔS with slope of one indicates complete enthalpy–entropy compensation which is indicative of reorganization of solvent molecules in quadruplex–ligand interactions [82]. Total enthalpy–entropy compensation occurs in systems with non-zero ΔC_p and $\Delta C_p > \Delta S$. The slope of ΔH versus temperature yields the ΔC_p value, which is −104.35 ± 16.07 cal/mol/K for H24–SGR interaction (Fig. 4C) and −151.54 ± 25.07 cal/mol/K for Pu27–SGR interaction (Fig. 4D).

The interaction of SGR with H24 and Pu27 duplex shows that SGR has a higher binding affinity for quadruplexes than the corresponding duplex sequences (Fig. S1A and B). Association constant for quadruplex is also higher than that evaluated for a random sequence such as ct DNA (Fig. S1C). Similar to the interaction with quadruplexes, the interaction with the duplexes is both enthalpically and entropically driven. Similar higher affinity for quadruplex binding as compared to duplex binding by small molecules has been reported earlier [83].

Table 2
Dissociation constant (determined by absorbance, fluorescence and ITC) and stoichiometry for the interaction of H24 and Pu27 with SGR in 10 mM potassium phosphate buffer (pH 6.8) containing 150 mM KCl.

System	Dissociation constant, K_d (μM) at 25 °C			Stoichiometry (Job Plot)
	Absorption	FPA	ITC	
H24–SGR	2.08	2.22 ± 0.42	1.56	1:2
Pu27–SGR	2.26	1.75 ± 0.03	3.62	1:3

3.3. Circular dichroism studies

CD experiments were done to examine any conformational changes that maybe induced in the quadruplex structure as a sequel to ligand binding. The CD spectrum of Pu27 is a characteristic of an all-parallel quadruplex structure with a major positive band at 260 nm and a minor negative band at 240 nm (Fig. 5A, *Spectrum 1*). Intensity of both peaks changes significantly upon complex formation with SGR (Fig. 5A and B). The presence of an isoelliptic point at 248 nm (Fig. 5A) suggests that a single type of complex forms between Pu27 and SGR. Induced CD band is found to be absent in the complex. CCA analysis shows that the CD spectra of Pu27 bound SGR can be deconvoluted into three basis spectra (Fig. 5C). One of these (component 1) is characteristic of the CD spectrum of Pu27. The other two components characterize the SGR bound form of Pu27. The variation of the associated coefficients of each basis spectra was plotted as a function of SGR concentration (Fig. 5D) which is characterized by (a) decrease in the percent population of component 1 (b) increase in

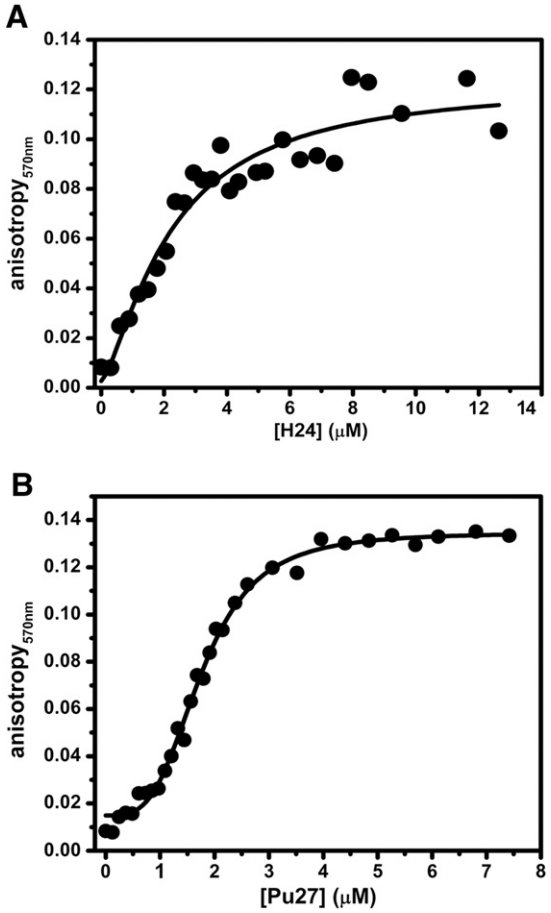

Fig. 3. Curve fitting analysis of the binding isotherm obtained from fluorescence anisotropy titration to evaluate the dissociation constant for the association of SGR with (A) H24 and (B) Pu27. 5 μM of SGR was titrated with increasing concentration of quadruplex at 25 °C in 10 mM potassium phosphate buffer (pH 6.8) containing 150 mM KCl (λ_{ex} = 327 nm, λ_{em} = 570 nm).

the percent population of component 3 and (c) increase followed by a decrease in the percent population of component 2. CD spectra of H24 on binding to SGR are characterized by a negative induced CD band at ~355 nm and a structural change from the (3 + 1) hybrid I to basket form (Na^+ form) at higher SGR concentrations [61].

3.4. Differential scanning calorimetric studies

To gain knowledge about the thermal stability of the quadruplexes in the presence and absence of SGR, DSC studies were performed. Successive melting profiles of both the bound and unbound forms of H24, Pu27, Pu121 and Pu161 overlapped indicating reversibility of the melting process. The thermodynamic melting parameters are summarized in Table 4 and Supplementary Table T1.

H24 melting is characterized by two major thermal transitions, one at 49.53 °C and the other at 66.17 °C (Fig. 6A). The observed melting transitions are consistent with earlier report [72]. The two melting transitions are shifted to higher temperatures in the complex, one at 76.55 °C and the other at 92.91 °C (Fig. 6C). The apparent excess enthalpy of transition increases from a total of 36.02 (10.68 + 25.34) kcal/mol in the unbound form to 72.74 (27.84 + 44.90) kcal/mol in the bound form. Our results differ from the report by Bhadra et al. [60] where an increase of only 9 °C is observed for H22 binding to SGR using optical melting and DSC techniques. FRET melting studies have shown that derivatives of berberine, an isoquinoline alkaloid with similar structure to SGR, impart quadruplex stability by increasing the melting temperature by 15 °C or more [49,55]. Since SGR has a completely planar structure as compared to berberine or its derivatives, it provides a better stacking interaction with the quartet plane resulting in higher ΔT_m values.

Pu27 melting is characterized by two major thermal transitions one at 79.32 °C and the other at 92.93 °C (Fig. 6B), which is in accordance with the theoretically calculated values (78.5 °C and 92.7 °C) from the empirical formulae

$$T_{m1} = 23.8 \times \log\left[K^+\right] + 26.7 \text{ and } T_{m2} = 24.4 \times \log\left[K^+\right] + 39.6$$

derived by Freyer et al. [84]. The melting transitions are shifted to higher temperatures in the complex, one at 105.9 °C and the other at 116.3 °C (Fig. 6D). The apparent excess enthalpy of transition increases from a total of 47.21 (13.44 + 33.77) kcal/mol in the unbound form to 61.41 (42.49 + 18.92) kcal/mol in the bound form.

While Pu27 shows two melting temperatures, the modified sequences, Pu161 and Pu121 show single melting temperatures at 78.89 (Fig. S2A) and 89.91 °C (Fig. S2B) respectively. The melting transitions are similar to those of 24 mer mutant c-myc sequence [85]. The melting transitions of the SGR bound forms are at 106.8 (Fig. S2C) and 116.1 °C (Fig. S2D) respectively. Comparison of the melting transitions of the SGR bound modified and wild type myc sequences indicates that the lower melting transition is for the 1:6:1 conformer while the higher melting transition is for the 1:2:1 conformer in SGR bound Pu27 [84,85].

3.5. Telomerase Repeat Amplification Protocol studies

TRAP is a sensitive technique which allows telomerase detection in mammalian cell and tissue extracts with very low telomerase activity levels. Our results show that as the concentration of SGR increases, the number of threshold cycles needed to obtain detectable fluorescence intensity increases which in turn leads us to conclude that SGR has an inhibitory effect on telomerase activity (Fig. 7). Our results are in accordance with a previous report which shows that SGR effectively blocks Taq polymerase.

4. Discussion

H24 (Table 1) sequence which we have used in the present study, folds predominantly into the (3 + 1) hybrid 1 conformer with minor amounts of (3 + 1) hybrid 2 in K^+ ions. The (3 + 1) hybrid structure has one double chain reversal loop and two edgewise loops [64,65,68]. The two hybrids differ in their loop arrangement. While the double chain reversal loop is the first loop in hybrid 1, it is the last loop in hybrid 2. Pu27 (Table 1) folds into an all-parallel quadruplex structure with three double chain reversal loops in K^+ ions [70,71]. There are five guanine stretches in the Pu27 sequence (Table 1) which can participate in the formation of the G-quartets [84,85]. These reports [84,85] have shown that in K^+ ions, this sequence adopts two structures, 1:2:1 conformer and 1:6:1 conformer, where the numbers indicate the number of bases in the loop region of the folded quadruplex containing three G-quartets. Here we have employed spectroscopic and calorimetric approaches to study the binding mode of SGR to two structurally different quadruplexes. The antitumor potential of SGR has received much attention from researchers in the recent past. Various mechanisms for the anticancer activity of SGR have been identified [86]. Our results suggest that interaction of SGR with quadruplex DNA which forms at the telomeric region and promoter of the c-myc oncogene might be one of the plausible mechanisms by which it imparts its anticancer activity.

Optical spectroscopic studies including CD provide direct evidence for the binding of SGR to quadruplexes. Change in absorption spectra of SGR on addition of quadruplexes is a direct evidence for complex formation (*Insets* of Fig. 2A and B). The observed red shift in the spectra can occur due to the stabilization of the π* orbital of SGR, thereby

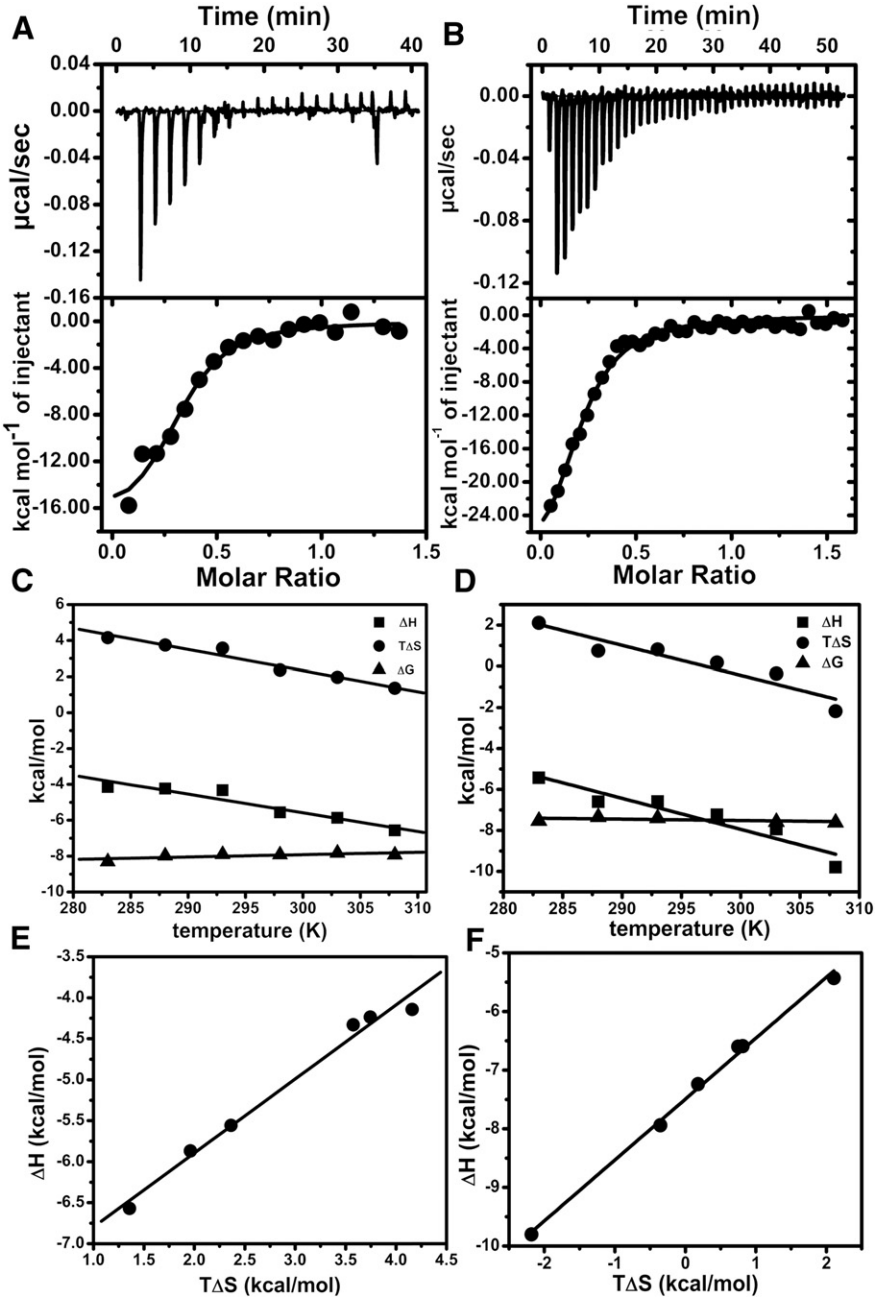

Fig. 4. Representative ITC profiles for the titration of (A) H24 and (B) Pu27 into a 10 μM solution of SGR in 10 mM potassium phosphate buffer (pH 6.8) containing 150 mM KCl at 25 °C. The upper panel shows the change in differential power (DP) of the instrument. Bottom panel shows the binding isotherm resulting from integration of the peak area as a function of molar ratio. The solid line represents the calculated fit of the data. Variation of thermodynamic parameters (ΔH: solid square, TΔS: solid circle, ΔG: solid triangle) for the association of SGR with (C) H24 and (D) Pu27 as a function of temperature. Linear temperature dependence of enthalpy yields ΔC_p. Enthalpy–entropy compensation plot for the interaction of SGR with (E) H24 and (F) Pu27.

reducing the energy gap for the π → π* transition [87,88]. Such stabilization could arise either from end stacking or intercalative mode of binding of planar SGR moiety to the G-quartets. Reduced quantum yield in the fluorescence emission spectra of SGR on binding to quadruplex could be due to the proximity of the molecule and the G-quartets upon binding. Such proximity results in the quenching of the singlet excited state of SGR as proposed earlier for the binding of other small molecules to quadruplexes [57,89]. Electron transfer reactions involving the ground state of guanine base as electron donor are responsible for such quenching [90]. There is an increase in the anisotropy value of SGR on binding to the quadruplexes (Fig. 3A and B). Increase in the anisotropy value of SGR on complex formation indicates restricted motion due to larger size of bound SGR as compared to free SGR. Change in anisotropy of free SGR in the presence of the quadruplexes was employed to determine the binding affinity values. They fall in the same range as determined from absorption spectroscopy and ITC studies (Table 2) thereby suggesting that they result from the association. Higher anisotropy of SGR in the complex with Pu27 as compared to H24 can be ascribed to two factors — (a) higher binding stoichiometry and (b) larger size of Pu27.

Comparison of the stoichiometry values (Table 2) indicates that Pu27 can accommodate one extra SGR molecule from a different mode of binding. Two SGR molecules bind to the two ends of H24 and Pu27. The third SGR molecule can bind either at the loop region

Table 3
Thermodynamic parameters for the association of H24 and Pu27 with SGR at various temperatures in 10 mM potassium phosphate buffer (pH 6.8) containing 150 mM KCl as determined by isothermal titration calorimetry (ITC).

System	T (K)	ΔH (kcal mol^{-1})	ΔS (cal mol^{-1} K^{-1})	ΔG (kcal mol^{-1})	$K_a \times 10^5$ (M^{-1})	ΔC_p (cal mol^{-1} K^{-1})	ΔG_{hyd} (kcal mol^{-1})
H24–SGR	283	−4.14 ± 0.19	14.70	−8.30	25.40 ± 1.06	−104.35 ± 16.07	−8.35 ± 1.66
	288	−4.24 ± 0.15	13.00	−7.98	11.50 ± 1.79		
	293	−4.33 ± 0.26	12.20	−7.90	7.82 ± 3.29		
	298	−5.56 ± 0.28	7.93	−7.92	6.40 ± 2.12		
	303	−5.87 ± 0.14	6.47	−7.83	4.41 ± 0.67		
	308	−6.57 ± 0.11	4.41	−7.93	4.20 ± 0.90		
Pu27–SGR	283	−5.43 ± 0.24	7.44	−7.54	6.57 ± 1.95	−151.54 ± 25.07	−12.12 ± 2.51
	288	−6.60 ± 0.42	2.60	−7.35	3.83 ± 0.96		
	293	−6.59 ± 0.28	2.78	−7.40	3.29 ± 0.90		
	298	−7.24 ± 0.20	0.60	−7.41	2.76 ± 0.49		
	303	−7.94 ± 0.16	−1.17	−7.59	2.95 ± 0.35		
	308	−9.80 ± 0.45	−7.08	−7.62	2.56 ± 0.73		

or the bases at the 5′ and 3′ ends of Pu27 which are not a part of the quadruplex core. Since SGR is an intercalator, the probability of its binding to the free bases at the two ends of the oligomer is unlikely. Also, earlier reports have shown that the loop region of Pu27 is a potential binding site for small molecules. We can thus speculate that along with end stacked SGR, Pu27 also has a SGR molecule attached to its loop region. Although we propose two potential binding regions for SGR binding to Pu27, the ITC thermograms could not be analyzed using the "two sets of sites" model. This model can be used for analyzing thermograms only if the binding affinities of the two sites are significantly different. Since our data could not be fit using the "two sets of sites" model we conclude that the binding affinity of SGR for end stacking and loop binding is comparable. Under these conditions, the reported association constant values for Pu27-SGR interaction as determined by ITC (Table 3) reflect an average of the binding affinities for both sites.

Similar 2:1 binding stoichiometry has been reported for SGR binding to H22 using NMR and molecular modeling studies [52]. Electrospray ionization mass spectrometric (ESI-MS) studies with several isoquinoline alkaloids have shown that they form 2:1 complexes with an mRNA quadruplex [91]. Crystal structure of human telomeric DNA with berberine shows the formation of a 2:1 complex [92] but solution studies have shown that a 1:1 complex formation occurs [56,60]. ESI-MS studies have shown that berberine forms a 2:1 complex with the parallel $[d(TGGGGT)]_4$ quadruplex. Berberine has a puckered structure due to ring unsaturation while nitidine and SGR has completely planar structures. Thus SGR and nitidine provide a better overlap with the quartet plane than berberine enabling a 2:1 stoichiometry for these molecules.

CD spectroscopy has become a very useful technique for detection and characterization of quadruplex DNA. SGR does not show any intrinsic optical activity, but upon binding to a chiral DNA molecule an induced CD band may emerge [60,61,93]. We have reported earlier that the CD spectrum of H24 changes upon binding to SGR at higher concentration of the molecule [61]. The SGR bound CD spectra of H24 is similar to the basket form rather than the (3 + 1) hybrid structure suggesting a structural transition at higher SGR concentrations. On the contrary, the CD spectra of Pu27 at higher SGR concentration indicate absence of any structural perturbation from the all-parallel arrangement suggesting that the SGR bound form also has an all-parallel quadruplex structure (Fig. 5A). CD peak intensity of Pu27 at 240 and 260 nm changes on binding to SGR (Fig. 5A and B). The decrease in the CD signals may occur due to (a) ligand-induced changes in the stacking interaction between the bases of quadruplex [94] and (b) disruption of the quadruplex structure as a sequel to ligand binding as reported for interaction of triarylpyridine ligand family with c-kit 1 and c-kit 2 [95] and TmPyP4 with a RNA G-quadruplex (M3Q) [96]. Enhanced melting temperature of the Pu27–SGR complex, as compared to free Pu27 as determined by DSC (Fig. 6B and D, Table 4), rules out the possibility of any structural disruption in the quadruplex upon SGR binding. The decrease in the CD intensities can thus be attributed to interaction between the chromophoric group of SGR and quartets of Pu27. While interaction of SGR with H24 leads to the formation of an induced CD (ICD) band at ~355 nm, no such ICD is formed in case of Pu27. The presence of flanking bases in Pu27 might be responsible for this observed difference [97]. Interestingly, the spectra of SGR bound Pu27 increase beyond 280 nm before tailing down to zero after 310 nm. This is the same region where SGR has substantial absorption. It has been reported that the determining factor for the CD spectra of G-quadruplexes is the polarity of the stacked quartets rather than the relative strand orientations of the backbone strands [98]. SGR bound to the loop region of Pu27 might result in polarity changes in the stacked quartet, which induces some antiparallel character in Pu27, keeping the overall fold of the quadruplex unchanged, leading to an increase in CD intensity beyond 280 nm. The experimental CD spectra for Pu27–SGR interaction could be deconvoluted into three basis spectra (Fig. 5C). Component 1 is the basis spectrum for free Pu27, component 2 is the basis spectrum for the SGR bound 1:2:1 Pu27 conformer and component 3 is the basis spectrum for the SGR bound 1:6:1 Pu27 conformer. Both these conformers are parallel quadruplexes with characteristic CD peaks at 260 and 240 nm as SGR binding does not induce any structural alteration from the all-parallel arrangement. Variation of the percentage population of the three components with SGR concentration (Fig. 5D) indicates that at lower SGR concentrations, 1:2:1 conformer bound form is the major population but as the SGR concentration increases, 1:6:1 bound conformer becomes the major form. Results from DSC studies (Table 4) also corroborate that the 1:6:1 conformer is the major component upon SGR binding. SGR binding imparts greater stability to 1:6:1 conformer (leading to a greater ΔT_m value) than to 1:2:1 conformer. It results in a concomitant transition from 1:2:1 conformer to 1:6:1 conformer. CD studies indicate that SGR at higher concentrations induces a structural transition in the mixed parallel–antiparallel quadruplex while keeping the structure of the parallel quadruplex unchanged.

ITC studies show that H24 has a higher free energy of binding hence affinity as compared to Pu27 for the entire temperature range (Table 3). The negative enthalpic contributions are indicative of non-covalent interactions like stacking, whereas the positive entropic contributions could be due to the release of water molecules and/or conformational changes in the quadruplex structure upon SGR binding [99,100]. Variation of enthalpy with temperature (Fig. 4C and D) indicates that the associations in both cases are characterized by large change in heat capacity values. Large negative ΔC_p for binding of SGR to the quadruplexes could be attributed to (a) burial of water accessible hydrophobic surface area, which gives rise to the release of bound water and/or the release of counter ions [99,100] and (b) destacking of bases in the loop regions of the quadruplexes as a sequel to the stacking interaction between the

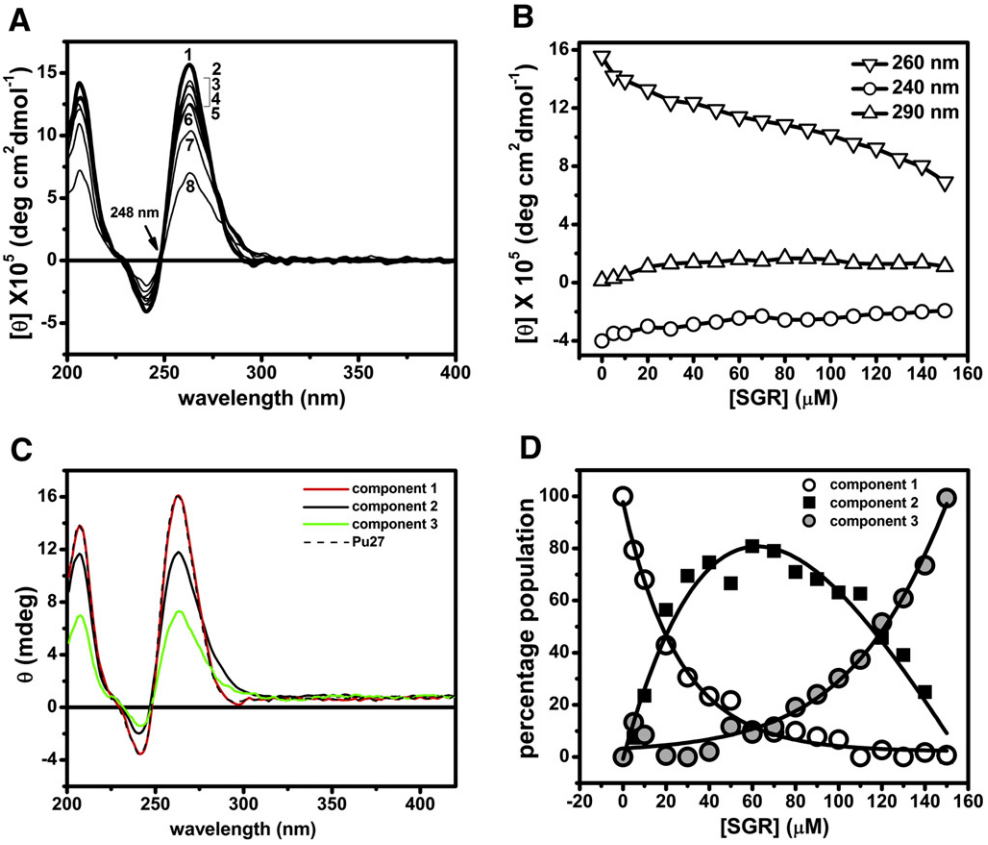

Fig. 5. (A) Representative CD spectra resulting from the interaction of Pu27 (10 μM, spetrum 1) with increasing SGR concentration (spectra 2–8 denotes 5, 10, 20, 30, 40, 100 and 150 μM of SGR) in 10 mM potassium phosphate buffer (pH 6.8) containing 150 mM KCl at 25 °C. (B) Variation in the molar ellipticity value at three selected wavelengths; 240, 260 and 290 nm for Pu27 SGR interaction. (C) Basis spectra obtained from CCA analysis of CD spectra shown in A and (D) Contribution of CCA components as a function of SGR concentration.

planar SGR moiety and G-quartets [101]. High ΔC_p values indicate a greater contribution of ΔG_{hyd} as evident from the following relation [102]

$$\Delta G_{hyd} = (80 \pm 10) \times \Delta C_p.$$

The binding of three SGR molecules to Pu27 results in release of greater number of bound water molecules as compared binding of two SGR molecules to H24. Thus the association of SGR with Pu27 has a greater ΔC_p and hence ΔG_{hyd} value (Table 3).

In case of systems with large ΔC_p values, T_H and T_S, the temperature limits beyond which the reaction is solely governed by enthalpy or entropy factors provide valuable information [103]. Within these temperature limits, both enthalpy and entropy factors govern the interactions. Our calculations show that for H24-SGR interaction, the limits are −25.7 °C and 45.5 °C respectively while for Pu27-SGR interaction, the limits are −22.9 °C and 25.4 °C respectively. Difference in T_s *i.e.* the temperature above which the reaction is solely enthalpically driven, is probably due to difference in the structure of the two quadruplexes which in turn results in SGR imparting different degrees of stability to both on binding. This indicates that the molecular basis of interaction in the two systems is not similar. It has been shown earlier that end-stacking interaction of H24 with small molecules leads to destacking of adenine bases in the loop region of H24 leading to the association being entropically favorable [101]. NMR reports on SGR-H24 interaction have shown that SGR binds to H24 by end stacking mode [61]. Association of SGR with H24 in an end stacking manner results in destacking of the adenine bases in the loop which probably leads to the association being favored entropically even at higher temperatures. SGR probably stacks on the G-quartets and also bind in the loop region of Pu27 as has been reported for the binding of many planar small molecules. As has been discussed later, SGR binds to the 1:6:1

Table 4
Thermodynamic parameters for intramolecular quadruplex to random coil transition, in the absence and presence of saturating concentration of SGR, for H24 and Pu27 in 10 mM potassium phosphate buffer (pH 6.8) containing 150 mM KCl as determined by differential scanning calorimetry (DSC).

System	T_{m1} (°C)	ΔH_{cal1} (ΔH_{v1}) (kcal mol^{-1})	ΔS_1 (cal mol^{-1} K^{-1})	$\Delta G_1^{25\ °C}$ (kcal mol^{-1})	T_{m2} (°C)	ΔH_{cal2} (ΔH_{v2}) (kcal mol^{-1})	ΔS_2 (cal mol^{-1} K^{-1})	$\Delta G_2^{25\ °C}$ (kcal mol^{-1})
H24 (100 μM)	49.53 ± 0.17	10.68 ± 0.17 (30.72 ± 0.33)	33.03	0.84	66.17 ± 0.02	25.34 ± 0.15 (56.48 ± 0.20)	74.70	3.03
H24 + SGR (70 μM + 190 μM)	76.55 ± 0.68	27.84 ± 1.31 (28.40 ± 0.74)	78.88	4.33	92.91 ± 0.05	44.90 ± 1.16 (63.02 ± 0.86)	122.40	8.42
Pu27 (100 μM)	79.32 ± 0.74	13.44 ± 0.98 (36.75 ± 1.09)	38.10	2.09	92.93 ± 0.07	33.77 ± 0.94 (60.41 ± 0.71)	92.24	6.28
Pu27 + SGR (70 μM + 260 μM)	105.9 ± 0.34	42.49 ± 1.49 (49.42 ± 0.79)	110.01	9.71	116.3 ± 0.08	18.92 ± 1.34 (104.0 ± 3.60)	48.07	4.60

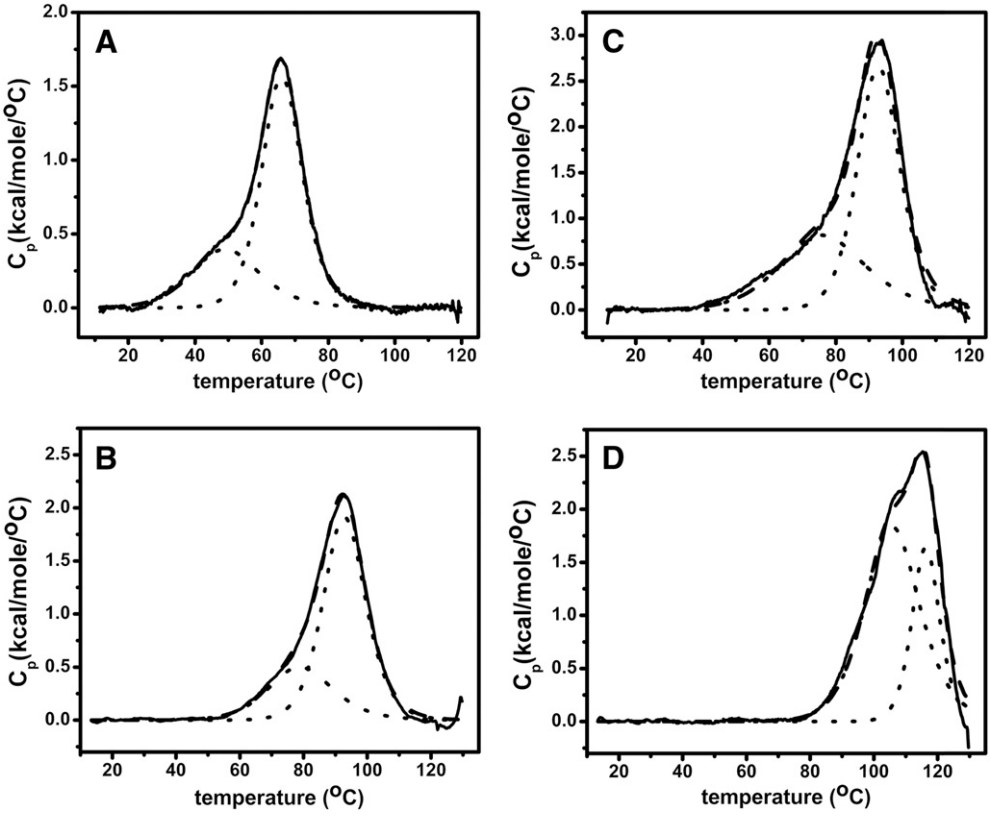

Fig. 6. Excess heat capacity profile for 100 μM (A) H24 and (B) Pu27 in absence of SGR and 70 μM (C) H24 and (D) Pu27 in the presence of saturating SGR concentrations (190 μM and 260 μM respectively) in 10 mM potassium phosphate buffer (pH 6.8) containing 150 mM KCl. The observed data (solid line) were deconvoluted (dotted lines) using the inbuilt "2-state" model for curve fitting software. The dashed curve denotes the overall fit of the data.

Pu27 isomer preferentially, shifting the equilibrium between the two conformers towards the 1:6:1 isomer. Binding of SGR to the loop region of 1:6:1 isomer of Pu27 reduces the flexibility of bases in the loop region leading to ordering of the system. This might result in the association being unfavorable at higher temperatures. The higher binding affinity of SGR for quadruplexes as compared to the corresponding duplexes and ct DNA (Fig. S1) indicates that SGR exhibits selectivity for binding to these structures over duplex DNA.

It has been suggested earlier that all-parallel quadruplexes are thermodynamically more stable than either the mixed parallel–antiparallel or antiparallel quadruplexes [13,104]. The higher melting temperature of unbound Pu27 as compared to unbound H24 could be due to the all-parallel structure that Pu27 adopts as compared to the mixed parallel–antiparallel structure adopted by H24 (Fig. 6A and B, Table 4). Three state melting process of H24 corroborates with previous results from Antonacci et al. [72]. The process is characterized by the gradual disappearance of one species, gradual appearance of the second species and concerted formation and disappearance of the transient species. Involvement of a transient species in the melting process results in $\Delta H_{VH} \neq \Delta H_{cal}$ [105]. SGR binding to H24 increases the melting temperature and the total enthalpy of transition indicating that SGR stabilizes H24 (Fig. 6C, Table 4). While the first melting transition is characterized by almost equal van't Hoff and calorimetric heat change ($\Delta H_{VH} / \Delta H_{cal} = 1.02$) the second melting transition has $\Delta H_{VH} / \Delta H_{cal} = 1.40$. CD and lifetime results reported earlier have shown that above 2:1 molar ratio of SGR, H24 undergoes a structural alteration [61]. Since the DSC profile of the bound form is reported at a molar ratio of 2.7:1, it is expected that a mixed population of SGR bound H24 will be present. The two melting transitions are most probably due to the two bound species. One of these undergoes a one step melting process with no involvement of any intermediate species while the melting of the other form involves an intermediate. But present data is insufficient to assign the transitions to any particular form.

In case of Pu27 the two melting temperatures correspond to the melting of the two conformers which co-exist at room temperature (Fig. 6B, Table 4). There have been reports which show that as the number of bases in the loop region increases, the melting temperature of the quadruplex decreases [13,104]. Thus it can be suggested that the lower melting transition is for the 1:6:1 conformer while the higher transition is for the 1:2:1 conformer [84,85]. In the unbound form, the apparent excess enthalpy for the melting of the 1:6:1 conformer contributes about 28.4% while the 1:2:1 conformer contributes about 71.6% of the total enthalpy change involved in the melting process. This indicates that at room temperature the 1:2:1 conformer is the major form in which Pu27 folds. The melting

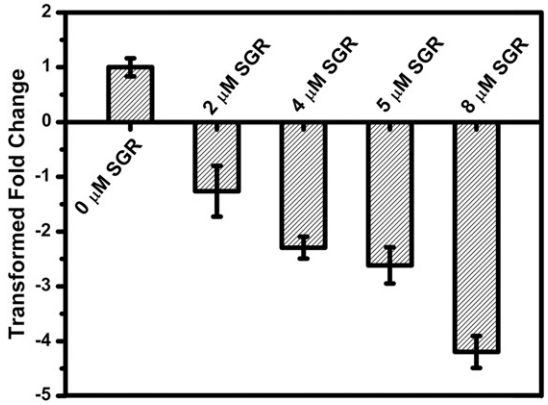

Fig. 7. TRAP assay using RT-PCR to determine the concentration dependent change of telomerase activity on extracts from MDAMB-231 cell line. The experiments were run in triplicates with 0, 2, 4, 5 and 8 μM SGR.

temperatures of both the modified Pu27 sequences (Fig. S2A and B, Table 1 and Supplementary Table T1) are in close resemblance with the two melting transitions of Pu27 indicating that the two forms are indeed present in Pu27. SGR binding to Pu27 increases the melting temperature and the total enthalpy of transition indicating that SGR stabilizes Pu27 (Fig. 6D, Table 4). Earlier reports have indicated that 1:6:1 conformer has a higher propensity to bind to small molecules than the 1:2:1 conformer and the former complex is more stabilized than the latter [84]. Comparison of the melting transitions of the SGR bound unmodified and modified c-myc sequences (Table 4 and Supplementary Table T1), allowed us to identify the transition temperatures of the bound form in the unmodified sequence. Greater ΔT_m value for the 1:6:1 conformer indicates that although this isomer melts at a lower temperature it is more stabilized than the 1:2:1 isomer upon SGR binding. This is in accordance with earlier reports. In the bound form, the apparent excess enthalpy for the melting of the 1:6:1 conformer contributes about 69.2% while the 1:2:1 conformer contributes about 30.8% of the total enthalpy change involved in the melting process. The enhanced stability of the 1:6:1 conformer on SGR binding and greater contribution of the SGR bound form towards enthalpy change of the melting of the Pu27–SGR complex, indicates that, the 1:6:1 conformer binds preferentially to SGR shifting the equilibrium between the two conformers more towards the 1:6:1 conformer. This is also in accordance with the CD results, where CCA analysis (Fig. 5D) suggests that, the 1:6:1 isomer, which was initially the minor component in Pu27, becomes the major component upon association with SGR. $\Delta H_{VH} / \Delta H_{cal} > 1$ for the melting of free Pu27 and 1:2:1 bound conformer indicates that the melting process involves intermediate species. But the melting of 1:6:1 bound conformer is a one step process. $\Delta H_{VH} / \Delta H_{cal} > 1$ indicates that end-to-end aggregates might be present possibly due to the aggregating tendency of guanine residues [105].

The interaction of a 22 nucleotide human telomeric DNA sequence, 5′-[AGGG(TTAGGG)$_3$]-3′ (H22) in K^+ ions, with SGR has been reported earlier by Bhadra et al. [60]. This report lacks an in-depth investigation of the structural basis of recognition of quadruplex by SGR using different techniques. It merely reports the affinity constant of the association between H22 and SGR. In addition it may be noted that several studies have shown that H22 folds into an assemblage of mixed parallel–antiparallel structures where along with the (3 + 1) hybrid forms, chair and basket conformers are also present [66,106].

Results from TRAP assay (Fig. 7) indicate that SGR binds to the quadruplex that forms at the end of the template primer and blocks the activity of telomerase, thereby inhibiting further elongation of the DNA template as the PCR cycle progresses. TRAP assay which allows us to quantitate the telomerase activity directly is a more sensitive technique to detect telomerase activity as compared to Taq assay. Though difficult to quantitate, the report by Bai et al. [107] where Taq assay was used to demonstrate SGR inhibits telomerase activity shows that even at 30 μM SGR concentration telomerase activity is not completely inhibited. In our study we see that as the concentration of SGR increases from 2 μM to 8 μM the telomerase activity decreases from 21% to 76% as compared to the control set (SGR concentration = 0 μM where telomerase activity is 100%). Our results indicate that SGR can effectively inhibit telomerase activity at a much lower concentration than thought of earlier based on data available from Taq assay.

A previous study from our laboratory showed that SGR does not inhibit *in vitro* transcription of DNA template but inhibits acetylation dependent chromatin transcription in a concentration dependent manner [59]. A recent paper by Sun et al. [108], have shown that SGR inhibits c-myc transcription by inhibiting Stat3 by suppression of Jak2 and Src phosphorylation. Another probable mechanism for inhibiting c-myc transcription by SGR might be by direct stabilization of the promoter sequence upstream of the gene (sequence same as Pu27 used in this study). Our results propose that binding of SGR to the quadruplex structure stabilizes this region and hence it can directly inhibit c-myc transcription.

Currently, *in vivo* and *ex vivo* NMR studies in *Xenopus laevis* oocytes and natively crowded cell extract of *X. laevis* egg residue have shown that the d(AG$_3$(TTAGGG)$_4$) sequence folds predominantly into the hybrid 1 structure [109]. But if the number of G4 motifs are increased the hybrid 2 and 2-tetrad antiparallel basket structure becomes the predominant conformation [109]. It was shown recently that quadruplex structures are indeed formed at the telomeric regions of mammalian cells but the exact structure adopted by them *in vivo* is still not established [110]. Our current results and other reports show that SGR interacts and stabilizes the hybrid, parallel and antiparallel [52] quadruplexes. So, it has the potential as an effective quadruplex stabilizing agent. However, studies on ligand binding to quadruplex under *in vivo*/*ex vivo* conditions need be extended, because it will enhance our knowledge regarding their mechanism of action as anticancer agent.

5. Conclusion

G-quadruplex binding ligands can effectively act as potential anticancer agents by either interfering with telomere maintenance or by altering expression level of oncogenes. However, since non-specific binding of ligands to duplex DNA leads to acute and intolerable side effects in normal tissues, further efforts in drug design is necessary to increase the specificity of these ligands towards quadruplex structures. Also, drug design should aim at selectivity among different quadruplex structures, as these structures have been identified in an increasing number throughout the genome. Natural compounds with therapeutic potential would be ideal for developing into potential anticancer agents. In this study we have reported that SGR binds to both mixed parallel–antiparallel and all-parallel form but with higher affinity towards the former. It also induces a structural change from hybrid to basket form while maintaining the structure for parallel quadruplex. These results may be useful in improving the selectivity of SGR to bind to mixed quadruplex structure as compared to all-parallel quadruplex structure.

Acknowledgements

DDG acknowledges the financial assistance from an intramural grant, Molecular Mechanism of Diseases and Drug Action, Department of Atomic Energy, Govt. of India. SC acknowledges Research Grant from CSIR (HCP 004), India. AK acknowledges Senior Research Fellowship from CSIR, India.

Appendix A. Supplementary data

Supplementary data to this article can be found online at http://dx.doi.org/10.1016/j.bbagen.2013.03.027.

References

[1] M.M. Seidman, P.M. Glazer, The potential for gene repair *via* triple helix formation, J. Clin. Invest. 112 (2003) 487–494.
[2] F.A. Hays, J. Watson, P.S. Ho, Caution! DNA crossing: crystal structures of Holliday junctions, J. Biol. Chem. 278 (2003) 49663–49666.
[3] A. Bacolla, R.D. Wells, Non-B DNA conformations, genomic rearrangements, and human disease, J. Biol. Chem. 279 (2004) 47411–47414.
[4] S.H. Chou, K.H. Chin, A.H. Wang, Unusual DNA duplex and hairpin motifs, Nucleic Acids Res. 31 (2003) 2461–2474.
[5] S. Arnott, R. Chandrasekaran, C.M. Marttila, Structures for polyinosinic acid and polyguanylic acid, Biochem. J. 141 (1974) 537–543.
[6] M. Gellert, M.N. Lipsett, D.R. Davies, Helix formation by guanylic acid, Proc. Natl. Acad. Sci. U. S. A. 48 (1962) 2013–2018.
[7] S.B. Zimmerman, G.H. Cohen, D.R. Davies, X-ray fiber diffraction and model-building study of polyguanylic acid and polyinosinic acid, J. Mol. Biol. 92 (1975) 181–192.
[8] J.R. Williamson, G-quartet structures in telomeric DNA, Annu. Rev. Biophys. Biomol. Struct. 23 (1994) 703–730.
[9] S. Burge, G.N. Parkinson, P. Hazel, A.K. Todd, S. Neidle, Quadruplex DNA: sequence, topology and structure, Nucleic Acids Res. 34 (2006) 5402–5415.
[10] T.M. Ou, Y.J. Lu, J.H. Tan, Z.S. Huang, K.Y. Wong, L.Q. Gu, G-quadruplexes: targets in anticancer drug design, ChemMedChem 3 (2008) 690–713.

[11] A.T. Phan, V. Kuryavyi, D.J. Patel, DNA architecture: from G to Z, Curr. Opin. Struct. Biol. 16 (2006) 288–298.
[12] V. Dapic, V. Abdomerovic, R. Marrington, J. Peberdy, A. Rodger, J.O. Trent, P.J. Bates, Biophysical and biological properties of quadruplex oligodeoxyribonucleotides, Nucleic Acids Res. 31 (2003) 2097–2107.
[13] A.N. Lane, J.B. Chaires, R.D. Gray, J.O. Trent, Stability and kinetics of G-quadruplex structures, Nucleic Acids Res. 36 (2008) 5482–5515.
[14] W. Li, P. Wu, T. Ohmichi, N. Sugimoto, Characterization and thermodynamic properties of quadruplex/duplex competition, FEBS Lett. 526 (2002) 77–81.
[15] J. Feigon, K.M. Koshlap, F.W. Smith, 1H NMR spectroscopy of DNA triplexes and quadruplexes, Methods Enzymol. 261 (1995) 225–255.
[16] A.T. Phan, D.J. Patel, Differentiation between unlabeled and very-low-level fully ^{15}N,^{13}C-labeled nucleotides for resonance assignments in nucleic acids, J. Biomol. NMR 23 (2002) 257–262.
[17] J. Eddy, N. Maizels, Conserved elements with potential to form polymorphic G-quadruplex structures in the first intron of human genes, Nucleic Acids Res. 36 (2008) 1321–1333.
[18] E. Henderson, C.C. Hardin, S.K. Walk, I. Tinoco Jr., E.H. Blackburn, Telomeric DNA oligonucleotides form novel intramolecular structures containing guanine-guanine base pairs, Cell 51 (1987) 899–908.
[19] J.L. Huppert, S. Balasubramanian, G-quadruplexes in promoters throughout the human genome, Nucleic Acids Res. 35 (2007) 406–413.
[20] A.K. Todd, M. Johnston, S. Neidle, Highly prevalent putative quadruplex sequence motifs in human DNA, Nucleic Acids Res. 33 (2005) 2901–2907.
[21] P. Rawal, V.B.R. Kummarasetti, J. Ravindran, N. Kumar, K. Halder, R. Sharma, M. Mukerji, S.K. Das, S. Chowdhury, Genome-wide prediction of G4 DNA as regulatory motifs: role in *Escherichia coli* global regulation, Genome Res. 16 (2006) 644–655.
[22] A. Verma, K. Halder, R. Halder, V.K. Yadav, P. Rawal, R.K. Thakur, F. Mohd, A. Sharma, S. Chowdhury, Genome-wide computational and expression analyses reveal G-quadruplex DNA motifs as conserved cis-regulatory elements in human and related species, J. Med. Chem. 51 (2008) 5641–5649.
[23] V.K. Yadav, J.K. Abraham, P. Mani, R. Kulshrestha, S. Chowdhury, QuadBase: genome-wide database of G4 DNA — occurrence and conservation in human, chimpanzee, mouse and rat promoters and 146 microbes, Nucleic Acids Res. 36 (2008) D381–D385.
[24] R.K. Thakur, P. Kumar, K. Halder, A. Verma, A. Kar, J.-L. Parent, R. Basundra, A. Kumar, S. Chowdhury, Metastases suppressor NM23–H2 interaction with G-quadruplex DNA within c-MYC promoter nuclease hypersensitive element induces c-MYC expression, Nucleic Acids Res. 37 (2009) 172–183.
[25] M. Fry, Tetraplex DNA and its interacting proteins, Front. Biosci. 12 (2007) 4336–4351.
[26] N. Maizels, Dynamic roles for G4 DNA in the biology of eukaryotic cells, Nat. Struct. Mol. Biol. 13 (2006) 1055–1059.
[27] C. Schaffitzel, I. Berger, J. Postberg, J. Hanes, H.J. Lipps, A. Pluckthun, *In vitro* generated antibodies specific for telomeric guanine–quadruplex DNA react with *Stylonychia lemnae* macronuclei, Proc. Natl. Acad. Sci. U. S. A. 98 (2001) 8572–8577.
[28] K. Walsh, A. Gualberto, MyoD binds to the guanine tetrad nucleic acid structure, J. Biol. Chem. 267 (1992) 13714–13718.
[29] L.H. Hurley, DNA and its associated processes as targets for cancer therapy, Nat. Rev. Cancer 2 (2002) 188–200.
[30] S. Neidle, G. Parkinson, Telomere maintenance as a target for anticancer drug discovery, Nat. Rev. Drug Discov. 1 (2002) 383–393.
[31] J.F. Riou, G-quadruplex interacting agents targeting the telomeric G-overhang are more than simple telomerase inhibitors, Curr. Med. Chem. Anticancer Agents 4 (2004) 439–443.
[32] D.J. Bearss, L.H. Hurley, D.D. Von Hoff, Telomere maintenance mechanisms as a target for drug development, Oncogene 19 (2000) 6632–6641.
[33] Y. Qin, L.H. Hurley, Structures, folding patterns, and functions of intramolecular DNA G-quadruplexes found in eukaryotic promoter regions, Biochimie 90 (2008) 1149–1171.
[34] T.A. Brooks, L.H. Hurley, The role of supercoiling in transcriptional control of MYC and its importance in molecular therapeutics, Nat. Rev. Cancer 9 (2009) 849–861.
[35] V. Gonzalez, L.H. Hurley, The c-MYC NHE III(1): function and regulation, Annu. Rev. Pharmacol. Toxicol. 50 (2010) 111–129.
[36] A. Siddiqui-Jain, C.L. Grand, D.J. Bearss, L.H. Hurley, Direct evidence for a G-quadruplex in a promoter region and its targeting with a small molecule to repress c-MYC transcription, Proc. Natl. Acad. Sci. U. S. A. 99 (2002) 11593–11598.
[37] T. Simonsson, P. Pecinka, M. Kubista, DNA tetraplex formation in the control region of c-myc, Nucleic Acids Res. 26 (1998) 1167–1172.
[38] T. Tomonaga, D. Levens, Activating transcription from single stranded DNA, Proc. Natl. Acad. Sci. U. S. A. 93 (1996) 5830–5835.
[39] I. Collins, A. Weber, D. Levens, Transcriptional consequences of topoisomerase inhibition, Mol. Cell. Biol. 21 (2001) 8437–8451.
[40] H. Arthanari, P.H. Bolton, Porphyrins can catalyze the interconversion of DNA quadruplex structural types, Anticancer Drug Des. 14 (1999) 317–326.
[41] M. Franceschin, L. Rossetti, A. D'Ambrosio, S. Schirripa, A. Bianco, G. Ortaggi, M. Savino, C. Schultes, S. Neidle, Natural and synthetic G-quadruplex interactive berberine derivatives, Bioorg. Med. Chem. Lett. 16 (2006) 1707–1711.
[42] M. Gunaratnam, O. Greciano, C. Martins, A.P. Reszka, C.M. Schultes, H. Morjani, J.F. Riou, S. Neidle, Mechanism of acridine-based telomerase inhibition and telomere shortening, Biochem. Pharmacol. 74 (2007) 679–689.
[43] F. Koeppel, J.F. Riou, A. Laoui, P. Mailliet, P.B. Arimondo, D. Labit, O. Petitgenet, C. Helene, J.L. Mergny, Ethidium derivatives bind to G-quartets, inhibit telomerase and act as fluorescent probes for quadruplexes, Nucleic Acids Res. 29 (2001) 1087–1096.
[44] E.M. Rezler, J. Seenisamy, S. Bashyam, M.Y. Kim, E. White, W.D. Wilson, L.H. Hurley, Telomestatin and diseleno sapphyrin bind selectively to two different forms of the human telomeric G-quadruplex structure, J. Am. Chem. Soc. 127 (2005) 9439–9447.
[45] J.F. Riou, L. Guittat, P. Mailliet, A. Laoui, E. Renou, O. Petitgenet, F. Megnin-Chanet, C. Helene, J.L. Mergny, Cell senescence and telomere shortening induced by a new series of specific G-quadruplex DNA ligands, Proc. Natl. Acad. Sci. U. S. A. 99 (2002) 2672–2677.
[46] J. Seenisamy, S. Bashyam, V. Gokhale, H. Vankayalapati, D. Sun, A. Siddiqui-Jain, N. Streiner, K. Shin-Ya, E. White, W.D. Wilson, L.H. Hurley, Design and synthesis of an expanded porphyrin that has selectivity for the c-MYC G-quadruplex structure, J. Am. Chem. Soc. 127 (2005) 2944–2959.
[47] T. Vy, Thi Le, S. Han, J. Chae, H.J. Park, G-quadruplex binding ligands: from naturally occurring to rationally designed molecules, Curr. Pharm. Des. 18 (2012) 1948–1972.
[48] C. Wei, J. Wang, M. Zhang, Spectroscopic study on the binding of porphyrins to (G(4)T(4)G(4))4 parallel G-quadruplex, Biophys. Chem. 148 (2010) 51–55.
[49] W.J. Zhang, T.M. Ou, Y.J. Lu, Y.Y. Huang, W.B. Wu, Z.S. Huang, J.L. Zhou, K.Y. Wong, L.Q. Gu, 9-Substituted berberine derivatives as G-quadruplex stabilizing ligands in telomeric DNA, Bioorg. Med. Chem. 15 (2007) 5493–5501.
[50] J.L. Zhou, Y.J. Lu, T.M. Ou, J.M. Zhou, Z.S. Huang, X.F. Zhu, C.J. Du, X.Z. Bu, L. Ma, L.Q. Gu, Y.M. Li, A.S. Chan, Synthesis and evaluation of quindoline derivatives as G-quadruplex inducing and stabilizing ligands and potential inhibitors of telomerase, J. Med. Chem. 48 (2005) 7315–7321.
[51] S. Ghosh, P. Majumder, S.K. Pradhan, D. Dasgupta, Mechanism of interaction of small transcription inhibitors with DNA in the context of chromatin and telomere, Biochim. Biophys. Acta 1799 (2010) 795–809.
[52] I. Bessi, C. Bazzicalupi, C. Richter, H.R. Jonker, K. Saxena, C. Sissi, M. Chioccioli, S. Bianco, A.R. Bilia, H. Schwalbe, P. Gratteri, Spectroscopic, molecular modeling, and NMR-spectroscopic investigation of the binding mode of the natural alkaloids berberine and sanguinarine to human telomeric G-quadruplex DNA, ACS Chem. Biol. 7 (2012) 1109–1119.
[53] Y. Ma, T.M. Ou, J.H. Tan, J.Q. Hou, S.L. Huang, L.Q. Gu, Z.S. Huang, Quinolino-benzo-[5, 6]-dihydroisoquindolium compounds derived from berberine: a new class of highly selective ligands for G-quadruplex DNA in c-myc oncogene, Eur. J. Med. Chem. 46 (2011) 1906–1913.
[54] P. Alberti, P. Schmitt, C.-H. Nguyen, C. Rivalle, M. Hoarau, D.S. Grierson, J.-L. Mergny, Benzoindoloquinolines interact with DNA tetraplexes and inhibit telomerase, Bioorg. Med. Chem. Lett. 12 (2002) 1071–1074.
[55] Y. Ma, T.-M. Ou, J.-H. Tan, J.-Q. Hou, S.-L. Huang, L.-Q. Gu, Z.-S. Huang, Synthesis and evaluation of 9-O-substituted berberine derivatives containing aza-aromatic terminal group as highly selective telomeric G-quadruplex stabilizing ligands, Bioorg. Med. Chem. Lett. 19 (2009) 3414–3417.
[56] A. Arora, C. Balasubramanian, N. Kumar, S. Agrawal, R.P. Ojha, S. Maiti, Binding of berberine to human telomeric quadruplex — spectroscopic, calorimetric and molecular modeling studies, FEBS J. 275 (2008) 3971–3983.
[57] H.J. Zhang, X.F. Wang, P. Wang, X.C. Ai, J.P. Zhang, Spectroscopic study on the binding of a cationic porphyrin to DNA G-quadruplex under different K^+ concentrations, Photochem. Photobiol. Sci. 7 (2008) 948–955.
[58] M. Zong-Wan, X.H. Zheng, Y.F. Zhong, C. Tan, L.N. Ji, Pt (II) squares as selective and effective human telomeric G-quadruplex binders and potential cancer therapeutics, Dalton Trans. 41 (2012) 11807–11812.
[59] B.R. Selvi, S.K. Pradhan, J. Shandilya, C. Das, B.S. Sailaja, G.N. Shankar, S.S. Gadad, A. Reddy, D. Dasgupta, T.K. Kundu, Sanguinarine interacts with chromatin, modulates epigenetic modifications, and transcription in the context of chromatin, Chem. Biol. 16 (2009) 203–216.
[60] K. Bhadra, G.S. Kumar, Interaction of berberine, palmatine, coralyne, and sanguinarine to quadruplex DNA: a comparative spectroscopic and calorimetric study, Biochim. Biophys. Acta 1810 (2011) 485–496.
[61] S.K. Pradhan, D. Dasgupta, G. Basu, Human telomere d[(TTAGGG)4] undergoes a conformational transition to the Na^+-form upon binding with sanguinarine in presence of K^+, Biochem. Biophys. Res. Commun. 404 (2011) 139–142.
[62] M. Maiti, G.S. Kumar, Molecular aspects on the interaction of protoberberine, benzophenanthridine, and aristolochia group of alkaloids with nucleic acid structures and biological perspectives, Med. Res. Rev. 27 (2007) 649–695.
[63] G.N. Parkinson, M.P. Lee, S. Neidle, Crystal structure of parallel quadruplexes from human telomeric DNA, Nature 417 (2002) 876–880.
[64] K.N. Luu, A.T. Phan, V. Kuryavyi, L. Lacroix, D.J. Patel, Structure of the human telomere in K^+ solution: an intramolecular (3 + 1) G-quadruplex scaffold, J. Am. Chem. Soc. 128 (2006) 9963–9970.
[65] A.T. Phan, K.N. Luu, D.J. Patel, Different loop arrangements of intramolecular human telomeric (3 + 1) G-quadruplexes in K^+ solution, Nucleic Acids Res. 34 (2006) 5715–5719.
[66] Y. Xu, Y. Noguchi, H. Sugiyama, The new models of the human telomere d [AGGG(TTAGGG)3] in K^+ solution, Bioorg. Med. Chem. 14 (2006) 5584–5591.
[67] J. Li, J.J. Correia, L. Wang, J.O. Trent, J.B. Chaires, Not so crystal clear: the structure of the human telomere G-quadruplex in solution differs from that present in a crystal, Nucleic Acids Res. 33 (2005) 4649–4659.
[68] A.T. Phan, V. Kuryavyi, K.N. Luu, D.J. Patel, Structure of two intramolecular G-quadruplexes formed by natural human telomere sequences in K^+ solution, Nucleic Acids Res. 35 (2007) 6517–6525.
[69] J. Dai, M. Carver, D. Yang, Polymorphism of human telomeric quadruplex structures, Biochimie 90 (2008) 1172–1183.
[70] A. Ambrus, D. Chen, J. Dai, R.A. Jones, D. Yang, Solution structure of the biologically relevant G-quadruplex element in the human c-MYC promoter. Implications for G-quadruplex stabilization, Biochemistry 44 (2005) 2048–2058.

[71] R.I. Mathad, E. Hatzakis, J. Dai, D. Yang, c-MYC promoter G-quadruplex formed at the 5′-end of NHE III1 element: insights into biological relevance and parallel-stranded G-quadruplex stability, Nucleic Acids Res. 39 (2011) 9023–9033.
[72] C. Antonacci, J.B. Chaires, R.D. Sheardy, Biophysical characterization of the human telomeric (TTAGGG)4 repeat in a potassium solution, Biochemistry 46 (2007) 4654–4660.
[73] A. Kettani, A. Gorin, A. Majumdar, T. Hermann, E. Skripkin, H. Zhao, R. Jones, D.J. Patel, A dimeric DNA interface stabilized by stacked A. (G.G.G.G).A hexads and coordinated monovalent cations, J. Mol. Biol. 297 (2000) 627–644.
[74] S. Chakrabarti, D. Bhattacharyya, D. Dasgupta, Structural basis of DNA recognition by anticancer antibiotics, chromomycin A3, and mithramycin: roles of minor groove width and ligand flexibility, Biopolymers 56 (2001) 85–95.
[75] C.Y. Huang, Determination of binding stoichiometry by the continuous variation method: the Job plot, Methods Enzymol. 87 (1982) 509–525.
[76] J.R. Lakowicz, Principles of fluorescence spectroscopy, Springer, 2006.
[77] P. Aich, R. Sen, D. Dasgupta, Role of magnesium ion in the interaction between chromomycin A3 and DNA: binding of chromomycin A3-magnesium (2+) complexes with DNA, Biochemistry 31 (1992) 2988–2997.
[78] J.E. Ladbury, M.L. Doyle, Biocalorimetry 2, Applications Calorimetry in the Biological Sciences, The Sussex John Wiley & Sons, Ltd., 2004. 259.
[79] A. Perczel, M. Hollosi, G. Tusnady, G.D. Fasman, Convex constraint analysis: a natural deconvolution of circular dichroism curves of proteins, Protein Eng. 4 (1991) 669–679.
[80] D. Suh, J.B. Chaires, Criteria for the mode of binding of DNA binding agents, Bioorg. Med. Chem. 3 (1995) 723–728.
[81] C. Wei, G. Jia, J. Yuan, Z. Feng, C. Li, A spectroscopic study on the interactions of porphyrin with G-quadruplex DNAs, Biochemistry 45 (2006) 6681–6691.
[82] J.B. Chaires, A thermodynamic signature for drug-DNA binding mode, Arch. Biochem. Biophys. 453 (2006) 26–31.
[83] A. Arora, S. Maiti, Effect of loop orientation on quadruplex — TMPyP4 interaction, J. Phys. Chem. B 112 (2008) 8151–8159.
[84] M.W. Freyer, R. Buscaglia, K. Kaplan, D. Cashman, L.H. Hurley, E.A. Lewis, Biophysical studies of the c-MYC NHE III1 promoter: model quadruplex interactions with a cationic porphyrin, Biophys. J. 92 (2007) 2007–2015.
[85] J.M. Dettler, R. Buscaglia, V.H. Le, E.A. Lewis, DSC deconvolution of the structural complexity of c-MYC P1 promoter G-quadruplexes, Biophys. J. 100 (2011) 1517–1525.
[86] J.-J. Lu, J.-L. Bao, X.-P. Chen, M. Huang, Y.-T. Wang, Alkaloids isolated from natural herbs as the anticancer agents, Evid. Based Complement. Alternat. Med. 2012 (2012) 485042–485054.
[87] M. Janovska, M. Kubala, V. Simanek, J. Ulrichova, Fluorescence of sanguinarine: spectral changes on interaction with amino acids, Phys. Chem. Chem. Phys. 12 (2010) 11335–11341.
[88] S. Lahiri, T. Takao, P.G. Devi, S. Ghosh, A. Ghosh, A. Dasgupta, D. Dasgupta, Association of aureolic acid antibiotic, chromomycin A3 with Cu^{2+} and its negative effect upon DNA binding property of the antibiotic, BioMetals 25 (2011) 1–16.
[89] H. Zhang, X. Xiao, P. Wang, S. Pang, F. Qu, X. Ai, J. Zhang, Conformational conversion of DNA G-quadruplex induced by a cationic porphyrin, Spectrochim. Acta A Mol. Biomol. Spectrosc. 74 (2009) 243–247.
[90] R. Jasuja, D.M. Jameson, C.K. Nishijo, R.W. Larsen, Singlet excited state dynamics of tetrakis (4-N-methylpyridyl) porphine associated with DNA nucleotides, J. Phys. Chem. B 101 (1997) 1444–1450.
[91] W. Tan, G. Yuan, Electrospray ionization mass spectrometric exploration of the high-affinity binding of three natural alkaloids with the mRNA G-quadruplex in the BCL2 5′-untranslated region, Rapid Commun. Mass Spectrom. 27 (2013) 560–564.
[92] C. Bazzicalupi, M. Ferraroni, A.R. Bilia, F. Scheggi, P. Gratteri, The crystal structure of human telomeric DNA complexed with berberine: an interesting case of stacked ligand to G-tetrad ratio higher than 1:1, Nucleic Acids Res. 41 (2013) 632–638.
[93] S. Das, G.S. Kumar, M. Maiti, Conversions of the left-handed form and the protonated form of DNA back to the bound right-handed form by sanguinarine and ethidium: a comparative study, Biophys. Chem. 76 (1999) 199–218.
[94] J.H. Fan, E. Bochkareva, A. Bochkarev, D.M. Gray, Circular dichroism spectra and electrophoretic mobility shift assays show that human replication protein A binds and melts intramolecular G-quadruplex structures, Biochemistry 48 (2009) 1099–1111.
[95] Z.A. Waller, S.A. Sewitz, S.T. Hsu, S. Balasubramanian, A small molecule that disrupts G-quadruplex DNA structure and enhances gene expression, J. Am. Chem. Soc. 131 (2009) 12628–12633.
[96] M.J. Morris, K.L. Wingate, J. Silwal, T.C. Leeper, S. Basu, The porphyrin TmPyP4 unfolds the extremely stable G-quadruplex in MT3-MMP mRNA and alleviates its repressive effect to enhance translation in eukaryotic cells, Nucleic Acids Res. 40 (2012) 4137–4145.
[97] E. Galezowska, A. Masternak, B. Rubis, A. Czyrski, M. Rybczynska, T.W. Hermann, B. Juskowiak, Spectroscopic study and G-quadruplex DNA binding affinity of two bioactive papaverine-derived ligands, Int. J. Biol. Macromol. 41 (2007) 558–563.
[98] S. Masiero, R. Trotta, S. Pieraccini, S. De Tito, R. Perone, A. Randazzo, G.P. Spada, A non-empirical chromophoric interpretation of CD spectra of DNA G-quadruplex structures, Org. Biomol. Chem. 8 (2010) 2683–2692.
[99] I. Haq, Thermodynamics of drug–DNA interactions, Arch. Biochem. Biophys. 403 (2002) 1–15.
[100] J. Ren, T.C. Jenkins, J.B. Chaires, Energetics of DNA intercalation reactions, Biochemistry 39 (2000) 8439–8447.
[101] D.S. Pilch, C.M. Barbieri, S.G. Rzuczek, E.J. Lavoie, J.E. Rice, Targeting human telomeric G-quadruplex DNA with oxazole-containing macrocyclic compounds, Biochimie 90 (2008) 1233–1249.
[102] J.H. Ha, R.S. Spolar, M.T. Record Jr., Role of the hydrophobic effect in stability of site-specific protein–DNA complexes, J. Mol. Biol. 209 (1989) 801–816.
[103] R.L. Baldwin, N. Muller, Relation between the convergence temperatures Th^* and Ts^* in protein unfolding, Proc. Natl. Acad. Sci. U. S. A. 89 (1992) 7110–7113.
[104] C.C. Hardin, A.G. Perry, K. White, Thermodynamic and kinetic characterization of the dissociation and assembly of quadruplex nucleic acids, Biopolymers 56 (2000) 147–194.
[105] C.M. Olsen, W.H. Gmeiner, L.A. Marky, Unfolding of G-quadruplexes: energetic, and ion and water contributions of G-quartet stacking, J. Phys. Chem. B 110 (2006) 6962–6969.
[106] H. Sun, J. Xiang, Q. Li, Y. Liu, L. Li, Q. Shang, G. Xu, Y. Tang, Recognize three different human telomeric G-quadruplex conformations by quinacrine, Analyst 137 (2012) 862–867.
[107] L.P. Bai, M. Hagihara, Z.H. Jiang, K. Nakatani, Ligand binding to tandem G quadruplexes from human telomeric DNA, ChemBioChem 9 (2008) 2583–2587.
[108] M. Sun, C. Liu, N. Nadiminty, W. Lou, Y. Zhu, J. Yang, C.P. Evans, Q. Zhou, A.C. Gao, Inhibition of Stat3 activation by sanguinarine suppresses prostate cancer cell growth and invasion, Prostate 72 (2012) 82–89.
[109] R. Hänsel, F. Löhr, L. Trantirek, V. Dötsch, High-resolution insights into G-overhang architecture, J. Am. Chem. Soc. 135 (2013) 2816–2824.
[110] G. Biffi, D. Tannahill, J. McCafferty, S. Balasubramanian, Quantitative visualization of DNA G-quadruplex structures in human cells, Nat. Chem. 5 (2013) 182–186.